Journal of Computing and Electronic Information Management
ISSN: 2413-1660 | Vol. 10, No. 2, 2023

Research on the servo strategy of permanent magnet synchronous motor based on self-anti-disturbance control

Qiu Jin

School of Electrical Engineering, Southwest Minzu University, Chengdu, China

Abstract: A new servo system is designed based on the ADRC control mechanism and the mathematical model of the permanent magnet synchronous motor (PMSM), replacing the traditional PID controller with a speed loop controller and a current loop controller. The ADRC improves the immunity of the system to load disturbance, improves the robustness and control accuracy, and effectively suppresses the generation of current harmonics. The simulation results show that compared with the traditional PID-controlled servo system, the system has a faster response, smaller overshoot, and higher control accuracy when the load torque changes, and the system is almost unaffected when the internal parameters of the motor change.

Keywords: Permanent magnet synchronous motor; ADRC; PID controller; Speed loop control.

1. Introduction

PMSM have been widely used in modern AC drive systems due to their advantages of simple structure, high power density, high reliability, and easy maintenance, especially in robotics, aerospace, CNC machine tools, and other fields that require high motor performance and control accuracy [1-2]. However, PMSM is a typical nonlinear multivariable strongly coupled system, which is affected by external disturbances, parameter uptake and magnetic field nonlinearity, so the PMSM control system needs to be further optimized in terms of robustness and anti-disturbance [3-4]. Conventional PID controllers are "error-based feedback to eliminate errors" control methods, which can suppress constant or slow-varying disturbances to a certain extent [5]. However, if the whole system is to achieve a rapid, accurate, and micro-overshooting dynamic response to sudden load perturbations, the traditional PID controller cannot satisfy [6-7].

ADRC theory adopts the control idea of "disturbance feedforward compensation", which combines system input and output to achieve a reasonable distillation of system disturbance information, and compensates to the control system to achieve disturbance offset, so as to improve the system control performance [7-8]. At present, scholars at home and abroad have conducted a lot of research on ADRC. In the literature [9], a third-order linear ADRC is proposed to design the current loop, and the study shows that the control scheme has good current tracking and disturbance suppression performance, but there are problems such as excessive parameter gain. In [10], a nonlinear ADRC was proposed to design the current loop of the PMSM speed control system, but it has the shortcoming of difficult parameter tuning. In [11], a fractional-order integral control method is proposed to replace the state error feed-back control rate in ADRC, which has a better control effect, but the algorithm is too complex and difficult to be adjusted.

In this paper, we adopt ADRC control strategy to design PMSM speed-loop controller, improve the expanded state observer (ESO) part for the control characteristics of PMSM speed control system, and design the improved speed-loop self-rejecting controller (IADRC). Finally, the effectiveness of the control strategy is verified by simulation and experiment.

2. Mathematical model of PMSM

The PMSM is assumed to be an ideal motor, without losses and saturation, and the current is a three-phase symmetric sine wave [12]. Then, the stator voltage equation in d-q synchronous rotating coordinate system is

$$\begin{cases} u_d = R_s i_d + L_d \dfrac{di_d}{dt} - \omega_e \psi_q \\ u_q = R_s i_q + L_q \dfrac{di_q}{dt} + \omega_e \psi_d \end{cases} \tag{1}$$

Where: ud , uq are d and q axis voltages, respectively; id , iq are d and q axis currents, respectively; ψd , ψq are d and q axis magnetic chains, respectively; Ld , Lq are d and q axis inductances, respectively; ωe is the motor rotor electric angular velocity.

The equation of the motor stator magnetic chain is

$$\begin{cases} \psi_d = L_d i_d + \psi_f \\ \psi_q = L_q i_q \end{cases} \tag{2}$$

Where: ψf is the magnetic chain of permanent magnets.

The motor torque equation is given by

$$\begin{aligned} T_e &= 1.5 P_{\mathrm{n}} (\psi_d i_q - \psi_q i_d) = \\ & 1.5 P_n \left[\psi_f i_q + (L_d - L_q) i_d i_q \right] \end{aligned} \tag{3}$$

Where: Te is the electromagnetic torque; Pn is the number of motor pole pairs.

Taking the table-mounted permanent magnet synchronous motor as the object of study, there is Ld = Lq , and the control strategy of id = 0 is used, at which point equation (3) can be approximated and rewritten as follows

$$T_e = 1.5 P_n \psi_f i_q \tag{4}$$

The equation of motion of the motor is

$$T_e - T_L = J \frac{d\omega_m}{dt} + B\omega_m \tag{5}$$

Where: TL is the load torque; J is the rotational inertia; B is the viscous coefficient; ωm is the mechanical angular

velocity.

3. Speed control system ADRC design

3.1. Introduction to ADRC

A typical self-resistant controller consists of 3 parts, which are a tracking differentiator, an expansive state observer, and a nonlinear state error feedback control law. The structure is shown in Figure 1.

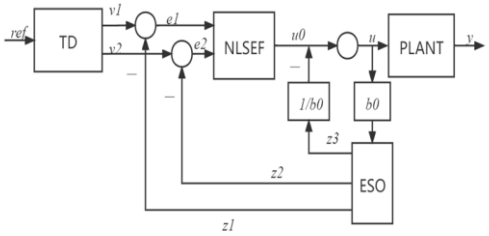

Fig. 1 ADRC structure

Among them, TD processes the input signal v to achieve a fast and overshoot-free tracking of the input signal by v1 , while v2 is the approximate differentiation of the input signal; ESO observes the real-time state variables of the system, z1 is the tracking signal of the output y, z2 is the approximate differentiation of the output y, and z3 is the observed value of the total system perturbation; v1 , v2 and z1 , z2 are differenced to obtain e1 , e2 as the input of the NLSEF, and in the NLSEF The corresponding output signal u0 is obtained by introducing an appropriate nonlinear function to process the input signal, and the system is transformed into a standard integrator series type system [13].

The second-order fastest discrete TD expression is as follows: where: v0 is the system input; x1 is the tracking value of the system input; x2 is the approximate differentiation of v:

$$\begin{cases} f_h = fhan(x_1 - v_0, x_2, r, h) \\ x_1(k+1) = x_1(k) + hx_2(k) \\ x_2(k+1) = x_2(k) + hf_h \end{cases} \tag{6}$$

The ESO formulation algorithm for the observation of second-order systems is as follows:

$$\begin{cases} \varepsilon = z_1 - y \\ \dot{z}_1 = z_2 - \beta_1 fal(\varepsilon, \alpha_1, \delta_1) \\ \dot{z}_2 = z_3 - \beta_2 fal(\varepsilon, \alpha_2, \delta_2) + b_0 u(t) \\ \dot{z}_3 = -\beta_3 fal(\varepsilon, \alpha_3, \delta_3) \end{cases} \tag{7}$$

In the above equation: e is the error valuation; y is the controlled object output value; z1 is the controlled object output estimate; z2 is the differential signal of z1; z3 is the estimated value of internal and external disturbances of the system; α1, α2, α3 are the nonlinear factors; β1, β2, β3 are the output error correction gains; b is the system disturbance compensation coefficient; δ is the filtering factor [12-14]. fal(e, α,δ) is expressed as follows:

$$\mathrm{fal}(e_1, \alpha, \delta) = \begin{cases} |e_1|^{\alpha}\mathrm{sign}(e_1) & |e_1| > \delta \\ \dfrac{e_1}{\delta^{1-\alpha}} & |e_1| \leqslant \delta \end{cases} \tag{8}$$

The NLSEF equation constituted by the selected fal function is as follows.

$$u_0 = \sum \beta_i fal(e_i, \alpha_i, \delta) \tag{9}$$

The non-linear combination of multiple reference quantities from TD and ESO real-time monitoring can significantly reduce the system steady-state error and avoid the steady-state high-frequency chattering.

The control volume after introducing perturbation estimation compensation:

$$u = \frac{u_0 - z_3}{b} \tag{10}$$

In summary, the ESO can be used to monitor and compensate the load changes synchronously, which can linearize the system dynamic compensation. Then, according to the separation principle of ADRC design, TD, ESO and NLSEF can be designed separately and combined into a complete ADRC.

3.2. TD design

The design equation for the speed loop TD is as follows:

$$\begin{cases} e_0 = v_1(k) - v_0 \\ v_1(k+1) = v_1(k) - h \cdot r \cdot fal(e_0, \alpha_0, \delta) \end{cases} \tag{11}$$

Where: v0 is the given speed or current; v1 (k) is the speed or current of the kth cycle of the actual operation;h is the value of the operation cycle;r is the value of the tracking speed decision.

3.3. ESO design

The design equation for the ESO of the speed ring is as follows:

$$\begin{cases} e_1 = z_1(k) - y \\ f_e = fal(e_1, \alpha_1, \delta) \\ a = z_2(k) - \beta_1 \cdot e_1 + b \cdot u \\ z_1(k+1) = z_1(k) + h \cdot a \\ z_2(k+1) = z_2(k) + h \cdot (-\beta_2 \cdot f_e) \end{cases} \tag{12}$$

Where: y is the detected system speed; z1 (k) is the system speed; z2 is the observed value of the internal and external disturbance for the whole speed loop; β1, β2 are the parameters of the speed or current observer.

3.4. NLSEF design

The speed loop NLSEF design equation is as follows, where β3 is the control gain of the speed loop

$$\begin{cases} e_2 = v_1(k) - z_1(k) \\ u_0 = \beta_3 fal(e_2, \alpha_2, \gamma) \end{cases} \tag{13}$$

The equation of the perturbation compensation process is as follows, where u is the control quantity of the final output of ADRC; b is the perturbation compensation coefficient, b = 1.2/L.

$$u = u_0 - \frac{z_2}{b} \tag{14}$$

Combining the above three parts, the final control output is achieved by the disturbance compensation process.

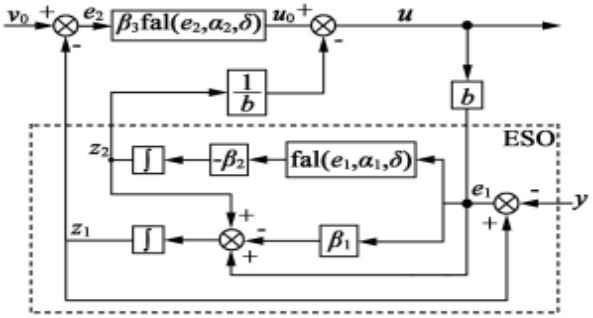

Fig. 2 First-order ADRC speed loop structure

4. Simulation and experimental results analysis

In this section, the rated speed response, anti-load torque disturbance speed response, response robustness under different speed settings and other motor performance indexes under rated speed with load are compared and analyzed for the PMSM speed loop under the traditional PI controller and nonlinear self-turbulent controller to verify the effectiveness and feasibility of the nonlinear self-turbulent controller and to show that the nonlinear self-turbulent The controller can make the motor speed response fast and overshoot-free, with better anti-load disturbance capability and good robustness of speed response than the traditional PI controller.

4.1. Simulink model building

To verify the effectiveness of the ADRC controller, the model is built in MATLAB/Simulink. Its basic block diagram is shown in Figures 3 and 4.

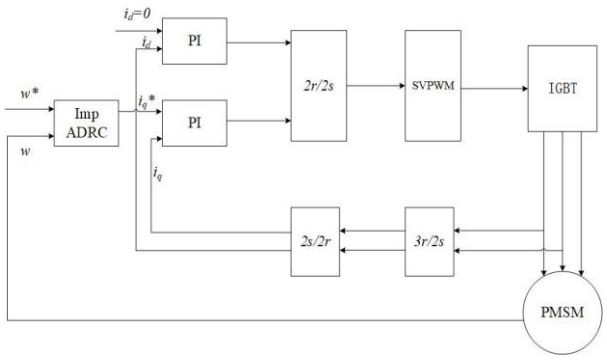

Fig. 3 Block diagram of PMSM control system based on self-anti-disturbance control

The parameters of the PMSM in the simulation are as follows: number of pole pairs Pn = 4; cross and straight axis inductance Ld = Lq = 6.5 mH, stator resistance Rs = 1.96 Ω , permanent magnet chain ψf = 0.23 Wb, rotational inertia J = 0.003 kg-m2 , viscous coefficient B = 0.008 N-m2 , rated speed 1000 r/s, and frontal voltage 311 V. To verify the above theory, this paper compares the conventional PI control with the ADRC-based controller. In order to verify the above theory, the conventional PI control is compared and analyzed with the ADRC-based controller.

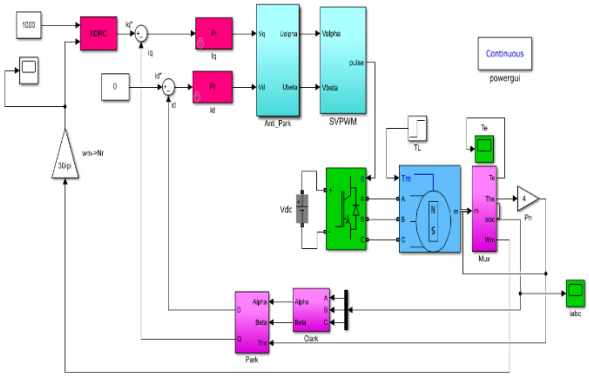

Fig. 4 Simulink simulation block diagram of ADRC closed-loop control system

4.2. Simulation results and analysis

The waveform comparison of the speed simulation results of ADRC and PI control in the rated speed response graph is shown below. Given a rated speed of 1000r/min, it can be seen that under ADRC control, the motor reaches the specified speed in 0.03s with no significant overshoot. The conventional PI controller has significant overshoot. Since the tracking differentiator in the speed loop ADRC controller arranges the transition process, the start-up speed under PI control is slightly higher than that under ADRC control. It is also due to the presence of the tracking differentiator that the contradiction between system response speed and overshoot is solved.

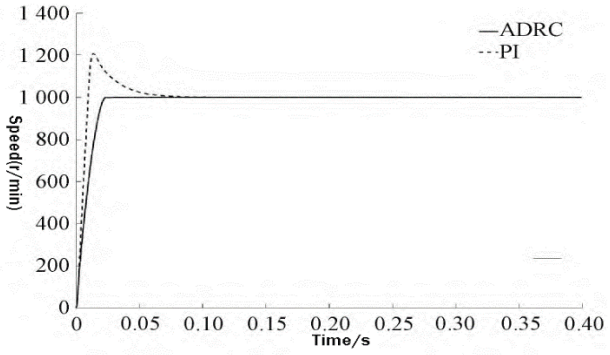

Fig. 5 Speed tracking waveform at rated speed

As shown in Fig. 6, in the experimental verification of the anti-disturbance of load torque, the absolute value of the speed fluctuation under the self-turbulent controller is much smaller than that of the PI controller when a load of 10 N-m is suddenly added at 0.2s with other parameters unchanged, and the recovery time to the rated speed is shorter, which indicates that the control strategy still has a good anti-disturbance performance with load.

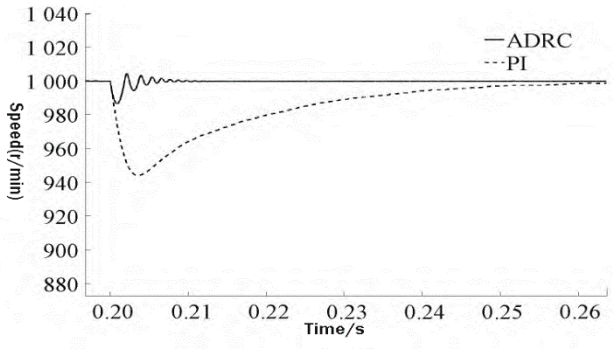

Fig. 6 Sudden load speed response waveform

In order to investigate the performance of the two controllers more deeply, the simulated waveforms of PMSM torque, d-axis current and three-phase current are compared under the two control strategies at rated speed with load, respectively. Figure 7 and Figure 8 show the comparison curves of the response waveforms of the motor electromagnetic torque and the output waveforms of the actual d-axis current of the motor under ADRC and conventional PI control, respectively.

As can be seen from the figure, the torque waveform under ADRC control is smoother and the starting maximum torque is smaller, showing better starting performance. d-axis current value fluctuates in the range of [-1,3], while the d-axis current value fluctuates in the range of [-4,4] for the conventional PI controller. Therefore, it can be seen from the figure that the actual performance of the d-axis current loop is better than that of the PI controller with the ADRC controller designed in this paper.

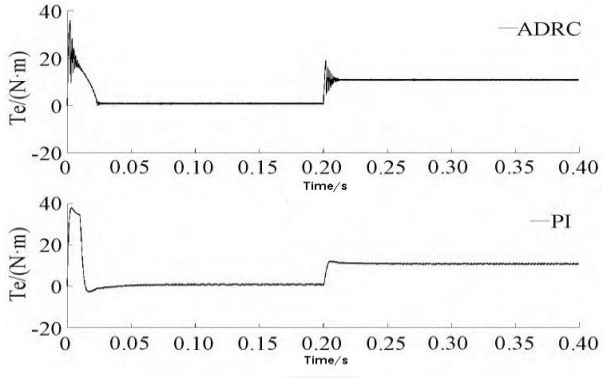

Fig. 7 Waveform of electromagnetic torque response under rated speed load

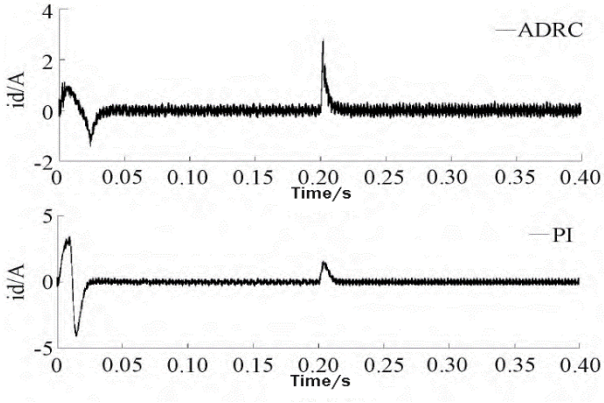

Fig. 8 Waveform of d-axis current under rated speed load

The actual output waveforms of the three-phase currents of the PMSM under the two control schemes of ADRC and PI are shown in Fig. 9. As can be seen from the figure, the peak three-phase currents are smaller under the ADRC controller designed in this paper, and the output waveforms of the three-phase currents are close to sinusoidal when the steady state is reached, which can better generate the rotating magnetic momentum.

The above experimental simulation results show that the ADRC-based PMSM speed control strategy proposed in this paper is more effective than the PI controller, which not only improves the anti-interference capability of the system and solves the contradiction between fast response and speed overshoot, but also has stronger robustness.

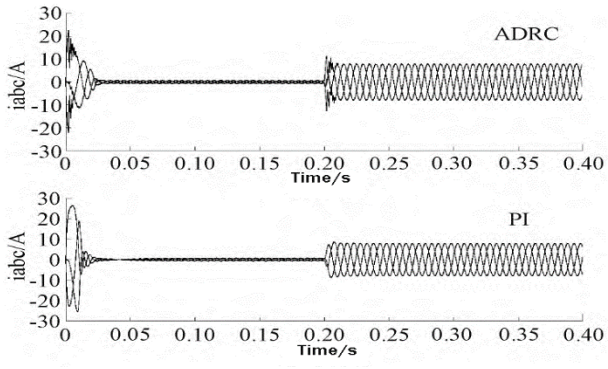

Fig. 9 PMSM three-phase current waveform under rated speed load

5. Conclusion

In this paper, from the perspective that the traditional PI-controlled PMSM servo system has a large overshoot in the speed response and poor anti-interference capability, the self-interference controller is introduced into the speed loop according to the self-interference control mechanism, and the general design method of a typical speed loop self-interference controller is given, and the self-interference control strategy is compared and studied with the traditional PI control strategy. Simulation and experimental results show that the self-turbulent controller proposed in this paper is applied to the speed loop and solves the problem of overshooting the speed response, and has a certain anti-disturbance capability and strong robustness. It shows that the control strategy has some practical application value and is an effective strategy for speed regulation of permanent magnet synchronous motor. However, this control strategy has room to improve the system response under the disturbance such as sudden load change, and the anti-disturbance ability still needs to be strengthened.

Acknowledgments

This work was financially supported by the Southwest Minzu University Graduate Innovative Research Project No. (YB2022428) fund.

References

[1] Xie Tao, Gao Guige, Wang Jie. Research on vector control system of PMSM based on sliding mode controller [J]. Motor and Control Applications, 2018, 45 (3) : 6.

[2] Cao Zhengze, Chu Yubo. Self-anti-disturbance based vector control system for permanent magnet synchronous motor [J]. Journal of Wuhan University (Engineering Edition), 2020, 53 (1): 67.

[3] Han Jingqing. Self-disturbance controller and its application [J]. Control and Decision Making, 1998, 13(1) : 19.

[4] Zhang Lei, Lu Kai, Tian Wei, et al. Design of variable gain self-anti-disturbance controller for permanent magnet synchronous motor servo system [J]. Microtechnology, 2020, 48 (8) : 35.

[5] WANG Gaolin, XU Jin, ZHANG Guoqiang, et al. Control strategy for direct-drive permanent magnet traction system without load cell [J]. China Journal of Electrical Engineering, 2015, 35(16): 4207.

[6] Liu Yaxuan. Research and implementation of a permanent magnet synchronous motor speed control system based on self-turbulence controller [D]. Guangzhou: Guangdong University of Technology, 2016.

[7] Hu Changling, Wang Dongping. PMSM vector control research [J]. Industrial Control Computer, 2020, 33(6): 155. [7] Han Jingqing. Self-disturbance control technology - control technology for estimating and compensating uncertainties [M]. Beijing: National Defense Industry Press, 2008.

[8] LIU H X, LI S H. Speed control for PMSM servo system using predictive functional control and extended stste observer [J]. IEEE Transactions on Industrial Electronecs, 2012, 59 (2): 1171 - 1183.

[9] Xie, Chuan-Lin, Zeng, Yue-Nan, Wang, Fa-Liang, et al. Design of PMSM speed loop self-turbulence controller based on disturbance compensation [J]. Microtechnology, 2017, 45 (12): 53-56.

[10] Liu, Chunqiang, Luo, Guangzhao, Tu, Wencong, et al. Self-anti-disturbance control based dual-loop servo system[J]. Chinese Journal of Electrical Engineering,2017,37(0):1-8.

[11] HAN J Q. From PID to active disturbance rejection control [J]. IEEE Transactions on Industrial Electronics, 2009, 56(3):900-906.

[12] Liu X.Y., Liao Y. Study on closed-loop control strategy of permanent magnet synchronous motor torque angle [J]. Microelectromechanics, 2011, 44(11):31-37.

[13] Lu D, Zhao G Z, Qu Y L, et al. Parameter-free rectification of permanent magnet synchronous motor with self-turbulence controller[J]. Journal of Electrotechnology, 2013, 28(3):27-34.